



### 1.1. Stages of Hydrate Formation

Natural gas hydrates form at the gas-liquid interfaces along the pipeline length at a static position. At this static position, small volumes of hydrate that cannot block the flow conduit are created with time. The gas hydrate formed does not become a threat to flow conduits until beyond the stage of

agglomeration where hydrate masses formed at the interface start bridging [6]. The bridging of these small accumulations of hydrates adheres to the walls of the pipeline, causing partial or complete pipeline blockage and hence reducing gas flow (Figure 2). This bridging can eventually shut down the entire pipeline until the hydrates have been removed.

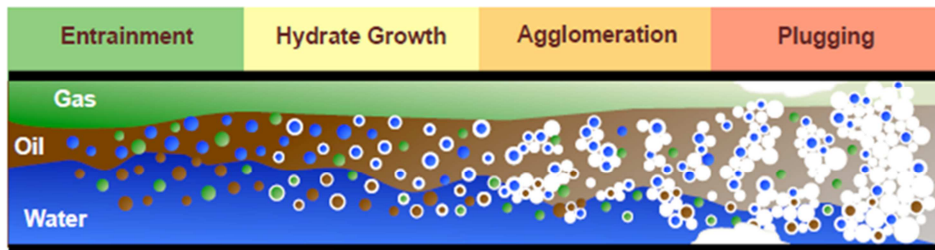


Figure 2. Image showing Hydrate growth processes (Source: Sum et al. [7]).

Predicting the point at which hydrates start to grow has been a challenge in the industry [8, 9]. This leads to the application of inhibitors at points in the flow where hydrate is yet to form; leading to wastage and increased costs; or the application of inhibitors at points where agglomeration rate is faster than inhibitor reaction rate thus affecting pipeline integrity and, also, increasing costs. When gas condensate is present in the pipeline, the prediction of the hydrate growth point is more complex and in some cases, leads to inhibitor pathway design errors.

In this paper, we put forward a model that predicts the point in the pipeline where hydrates start to form in the presence of condensate. This is done by predicting the temperature at which quasi liquid layer starts to form on the hydrate seed. Quasi liquid layer refers to a film of pure water that forms around the hydrate seeds at a particular temperature drop within the system [10, 11, 12]. When two seeds with this layer cluster together, they do so through “capillary bridging” – and the resulting crystal is bigger than the component seeds, thus leading to hydrate growth which eventually leads to the complete plugging of the pipeline with its consequential effects.

### 1.2. Causes of Hydrate Growth

The driving force for hydrate growth is the ‘joining’ together of smaller-sized hydrate nuclei. Once the nuclei keep coming together, the gas hydrate size keeps growing leading to agglomeration and plugging (Figure 2). If nuclei do not come together, the hydrate formed would be dispersed over the length of the pipeline and no agglomeration would occur [13]. So, what causes nuclei agglomeration? As temperature increases, a slim film of pure water forms around the hydrate. This film is known as Quasi-Liquid Layer or Pre-melting layer.

### 1.3. Pre-Melting Layer

When two blocks of gas hydrate cubes are brought together below the thermodynamic equilibrium dissociation temperature of the gas hydrate, the almost pure water film on either surface of the gas hydrate will merge and fill the gap between the two blocks [14]. The presence of a pre-melting

layer will increase the cohesive force between gas hydrate particles due to capillary bridging. As temperature decreases, gas hydrate dissociates spontaneously becoming water and guest gas that has been trapped in the clathrate structure. The guest gas will then become misty from the surrounding bulk gas medium, and the end result will be just a water film on the surface of the gas hydrate [14]. This pure water formed at the surface of the hydrates allows for stronger bonding [15]. According to Sloan [8], if two hydrate crystals with pre-melting layers touch, the two become one big mass with the layers of water moving through the capillary pores of the hydrate structure and forming a stronger bond. This means that the pre-melting layer encourages hydrate agglomeration.

## 2. Model Development

The thought process followed in the formulation of the model is given below:

- 1) Understanding microscopically, the processes that lead to hydrate formation and growth.
- 2) Understanding the crystal formation of hydrates, the energies involved in hydrate formation, and how to harness these energies to ensure that hydrate growth does not reach the point of agglomeration.
- 3) Understanding the pre-melting layer (or quasi-liquid layer) of hydrate crystals, temperature and pressure interactions that lead to quasi-liquid layer formation, and how best to keep these layers ‘repulsive’ so as not to encourage hydrate growth.
- 4) Accurately predicting hydrate behavior in the presence of condensate.

### 2.1. Microscopic Modelling of Hydrate Crystal Development

The hydrate formation process is synonymous with the crystallization process [16, 17]. As in crystallization, the hydrate formation process can be subdivided into a nucleation and growth process [16]. Hydrate nucleation is the process of forming critically-sized, stable hydrate nuclei, and hydrate growth is the process of development of these stable nuclei. Like all crystals,

hydrate structure obeys the law that crystals have as their atoms are arranged in a Bravais lattice. Bravais lattice refers to an infinite array of discrete points in a three-dimensional space [15, 18] and it can be described mathematically as:

$$R = n_1 a_1 + n_2 a_2 + n_3 a_3 + \dots \quad (1)$$

Where  $n_i$  is any integer and  $a_i$  are vectors that lie in different directions and span the lattice.

Because of this, nucleation occurs relatively slowly because initial crystal components must impinge on each other in correct orientation and placement. Thereafter, growth is much faster because crystals are added in a prearranged system. However, in the presence of a foreign object such as sand particles, nucleation is much faster because crystals fill up the void present in the foreign structure and then continue to grow (Figure 3) in a recognized pattern. This is heterogeneous nucleation.

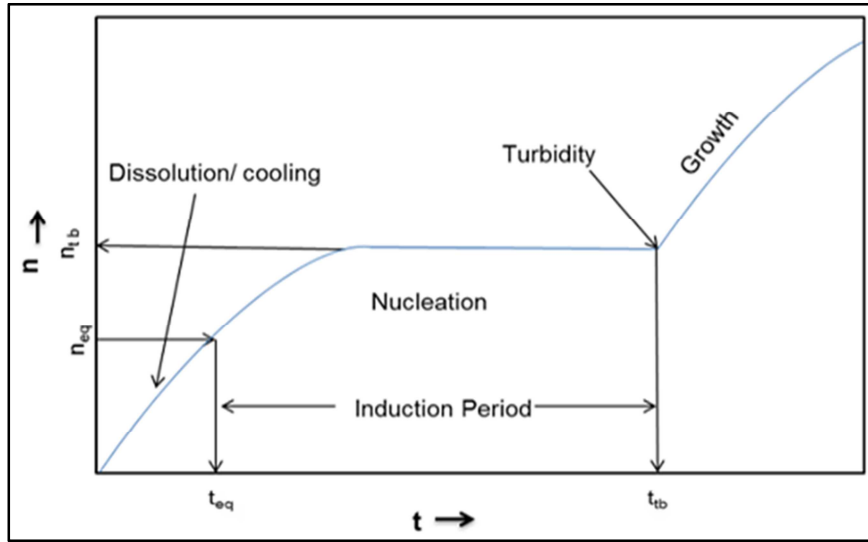


Figure 3. Hydrate growth processes in relation to time (Source: Kashchiev and Firoozabadi [19]).

Where  $n$  represents the number of moles of dissolved gas and  $t$  represents dissolution time.

### 2.1.1. For Homogeneous Nucleation

$$\Delta G_{hom} = \frac{4}{3}\pi r^3 G_v - 4\pi r^2 \sigma \quad (2)$$

where

$\Delta G_{hom}$  is the change of Gibbs free energy of the system upon dissolution of the particles if no impurities are present,

$G_v$  is the energy release due to the formation of solid per unit volume,

$r$  is the radius of hydrate nuclei and

$\sigma$  is the energy gain for the formation of a new surface per unit surface (interfacial energy).

### 2.1.2. For Heterogeneous Nucleation

However, heterogeneous nucleation is what is common in the field. The mathematical representation of this is

$$\Delta G_{het} = f(a, b, c) \Delta G_{hom} \quad (3)$$

Where  $f(a, b, c)$  is a correction factor, which depends on the contact angles  $a, b, c$  between the tangential line to the nuclei surface and the interphase which can only be gotten from experiments. The critical hydrate size, beyond which it can no longer be said to be in the nucleation stage is given by equation 4.

$$r_{critical} = \frac{2\sigma}{G_v} \quad (4)$$

Before critical hydrate size is reached, there is a force that seeks to prevent nucleation, this force is called the ‘free energy barrier’ represented by equation 5

$$\Delta G^* = \frac{16\pi\sigma^3}{3\Delta G_v} \quad (5)$$

The driving force for phase transformation is actually temperature change,  $\Delta T = T_m - T$ , where  $T_m$  is melting temperature and  $T$  is the current temperature of the mixture. In terms of temperature change, critical hydrate size and free energy barrier are given in equations 6 and 7, respectively.

$$r_{critical} = \frac{2\sigma T_m}{\Delta H_m \Delta T} \quad (6)$$

The free energy barrier [20] can also be written as

$$\Delta G^* = \frac{16\pi\sigma^3 T_m^2}{3\Delta(H_m)^2 \Delta T^2} \quad (7)$$

If  $\Delta G^* > \Delta G_{hom}$ , we can expect that there will be no hydrate formed. This is usually not the case because the energy barrier is strongly dependent on temperature as can be seen from equation 7. Also, temperature varies over the length of the pipeline.

## 2.2. Thermodynamic Modeling of Quasi-Liquid/ Pre-Melting Layer

It is known that the internal energy, U, that arises from the bonding between atoms/molecules favors crystalline structures while the entropy favors disorder [21]. From Gibbs free energy (G) the entropy (S) contribution to this is TS and the influence of the entropy term on G increases with temperature, T. Thus there is a temperature above which melting becomes favorable. The free energy at the surface and the thickness of the pre-melting layer are dependent on the temperature, the free energy at the surface of the hydrate, and the energy of dissociation that occurs when the temperature falls to  $T_m$ . This relationship as expressed by Nobuo [14], is given in equation (8).

$$\Delta G(h, \Delta T) = \frac{\Delta T}{T_m} \rho h \Delta H_{dissociation} + \Delta G_{surface} \quad (8)$$

Where:

$$\Delta G_{dissociation} = \frac{\Delta T}{T_m} H_{dissociation} = \Delta T \Delta S_{dissociation} \quad (9)$$

### 2.2.1. Quasi-Liquid Layer Formation Temperature

Seeing how important temperature variation is to the formation of the pre-melting layer (and hence hydrate agglomeration), in this study, we attempt to answer the

$$\frac{\partial}{\partial t} (\alpha_k \rho_k c_{p_k} T) + \frac{\partial}{\partial x} (\alpha_k \rho_k c_{p_k} u_k T) = -\alpha_k \left( \frac{d \ln \rho}{d \ln T} \right)_p \frac{Dp}{Dt} + \alpha_k \rho_k T \frac{Dc_{p_k}}{Dt} - \tau_{w_k} u_k + Q_k \quad (14)$$

Expanding the left hand side of equation 11 using product rule gives:

$$\frac{\partial}{\partial t} (\alpha_k \rho_k c_{p_k} T) = (\alpha_k \rho_k c_{p_k}) \frac{\partial T}{\partial t} + T \frac{\partial}{\partial t} (\alpha_k \rho_k c_{p_k}) \quad (15)$$

$$\frac{\partial}{\partial x} (\alpha_k \rho_k c_{p_k} u_k T) = (\alpha_k \rho_k c_{p_k} u_k) \frac{\partial T}{\partial x} + T \frac{\partial}{\partial x} (\alpha_k \rho_k c_{p_k} u_k) \quad (16)$$

Given that:

$$T \left( \frac{\partial}{\partial t} (\alpha_k \rho_k c_{p_k}) + \frac{\partial}{\partial x} (\alpha_k \rho_k c_{p_k} u_k) \right) = (\alpha_k \rho_k T) \frac{Dc_{p_k}}{Dt} \quad (17)$$

Substituting Equations 15, 16 and 17 into equation 14, simplifies the energy equation to:

$$(\alpha_k \rho_k c_{p_k}) \frac{\partial T}{\partial t} + (\alpha_k \rho_k c_{p_k} u_k) \frac{\partial T}{\partial x} = -\alpha_k \left( \frac{d \ln \rho}{d \ln T} \right)_p \frac{Dp}{Dt} - \tau_{w_k} u_k + Q_k \quad (18)$$

where  $C_p$  is the specific heat capacity,  $T$  is the temperature,  $Q$  is the heat transfer term,  $\tau_w$  is the shear stress acting on the wall of the pipe.

Since, hydrate formation does not constitute a threat to flow conduit integrity until the agglomeration stage, the following assumptions were made to further simplify the energy equation 18.

- 1) Heat transfer out of the system as a result of hydrate nuclei formation is negligible.
- 2) Shear stress acting on the walls of the pipe is negligible.

Hence, equation 18 becomes:

question, at what temperature change would the pre-melting layer occur? To answer this question, the first thing done was to model the thermodynamics of the system.

### 2.2.2. Mass Balance Equation

$$m_{total} = m_{gas} + m_{condensate} + m_{water} \quad (10)$$

Where:

$$m_{gas} = GCR \frac{m_{condensate}}{\rho_{condensate}} \rho_g \quad (11)$$

$$m_{water} = WC (q_{condensate} + q_w) \rho_w \quad (12)$$

$$m_{condensate} = m_{total} - (m_{gas} + m_{water})$$

$$m_{condensate} = \frac{m_{total}}{1 + GCR \frac{\rho_g}{\rho_{condensate}} + \frac{WC \rho_w}{(1-WC) \rho_{condensate}}} \quad (13)$$

### 2.2.3. Energy Balance Equation

The differential form of the energy equation in terms of time and space is:

$$\left(\alpha_k \rho_k c_{p_k}\right) \frac{\partial T}{\partial t} + \left(\alpha_k \rho_k c_{p_k} u_k\right) \frac{\partial T}{\partial x} = -\alpha_k \left(\frac{d \ln \rho}{d \ln T}\right)_p \frac{Dp}{Dt} \quad (19)$$

### 2.3. Temperature Change at Which Pre-Melting Layer Forms

The temperature at which pre-melting layer is formed is a function of both distance travelled and time. Solving the left hand side of the equation (19)

$$\left(\alpha_k \rho_k c_{p_k}\right) \frac{\partial T}{\partial t} + \left(\alpha_k \rho_k c_{p_k} u_k\right) \frac{\partial T}{\partial x} = B + R \quad (20)$$

Where B +R represents the solution to the equation i.e.

$$\left(\alpha_k \rho_k c_{p_k}\right) \frac{\partial T}{\partial t} = B \quad \text{and} \quad \left(\alpha_k \rho_k c_{p_k} u_k\right) \frac{\partial T}{\partial x} = R$$

Rearranging and integrating both equations:

$$\begin{aligned} \left(\alpha_k \rho_k c_{p_k}\right) \int_{T_1}^{T_2} dT &= B \int_{t_1}^{t_2} dt \\ \left(\alpha_k \rho_k c_{p_k}\right) (T_2 - T_1) &= B (t_2 - t_1) \end{aligned} \quad (21)$$

$$\left(\alpha_k \rho_k c_{p_k}\right) \Delta T = B \Delta t$$

$$\begin{aligned} \left(\alpha_k \rho_k c_{p_k} u_k\right) \int_{T_1}^{T_2} dT &= R \int_{x_1}^{x_2} dx \\ \left(\alpha_k \rho_k c_{p_k} u_k\right) (T_2 - T_1) &= R (x_2 - x_1) \end{aligned} \quad (22)$$

$$\left(\alpha_k \rho_k c_{p_k} u_k\right) \Delta T = R \Delta x$$

Hence the energy equation 16 becomes

$$\left(\alpha_k \rho_k c_{p_k}\right) (1 + u_k) \Delta T = B \Delta t + R \Delta x \quad (23)$$

Where ‘B’ and ‘R’ are empirical correlation constant.

Since, hydrate nuclei is already present in the flowline, but has not reached critical mass, i.e. has not reached growth stage. Therefore, the mass flowrate of the hydrate formed can be gotten as the difference of the total mass flowrate at the time of interest and total of the mass flowrate at the start of flow as shown in equations 24, 25 and 26.

$$\dot{m}_{total \text{ at the start of flow}} = \dot{m}_{gas} + \dot{m}_{condensate} + \dot{m}_{water} \quad (24)$$

$$\dot{m}_{total \text{ at the time of interest}} = \dot{m}_{gas} + \dot{m}_{condensate} + \dot{m}_{water} + \dot{m}_{hydrate} \quad (25)$$

Substitute equation (24) into equation (25), gives:

$$\dot{m}_{hydrate} = \dot{m}_{total \text{ at the time of interest}} - \dot{m}_{total \text{ at the start of flow}} \quad (26)$$

From thermodynamics

$$c_{p_{hydrate}} = \frac{\Delta H}{\dot{m}_{hydrate}} \quad (27)$$

Writing Equation (23) in terms of the hydrate phase gives:

$$\left(\alpha_{hydrate} \rho_{hydrate} c_{p_{hydrate}}\right)\left(1 + u_{hydrate}\right) \Delta T = B \Delta t + R \Delta x \tag{28}$$

Substituting equation (27) into equation (28) gives:

$$\left(\alpha_{hydrate} \rho_{hydrate} \frac{\Delta H}{\dot{m}_{hydrate}}\right)\left(1 + u_{hydrate}\right) \Delta T = B \Delta t + R \Delta x \tag{29}$$

Hence, Pre-Melting Layer Temperature  $\Delta T_Q$  is given as:

$$\Delta T_Q = \frac{\dot{m}_{hydrate} (B \Delta t + R \Delta x)}{\left(\alpha_{hydrate} \rho_{hydrate}\right)\left(1 + u_{hydrate}\right) \Delta H} \tag{30}$$

In the absence of experimental data, Leach’s [22] approximation of the empirical constants ‘B’ and ‘R’ were used in this study. The author approximates that the cation heats on the formation of  $XH_4$  groups (of which methane is a part) are 656KJ for each mol. Going from dimensional analysis and based on the energy estimations the constants B and R were gotten as 0.721KJ/Kg/m<sup>2</sup>/s and 0.73 KJ/Kg/m<sup>3</sup>, respectively.

### 3. Results and Discussion

The input data used in this study after Vinatovskaja [23] is as shown in Table 1, while Table 2 is the input parameters for equation (30). Observation from this field shows that hydrates are formed at about 1000m of flow.

The result in Table 3 revealed that once the change in temperature of the pre-melting layer ( $\Delta T_Q$ ) is higher than the temperature drop ( $\Delta T_P$ ) of the whole pipeline, it is expected that hydrates should start clumping together – that is growing. At a distance of 1000ft, it was observed that the temperature drop of the pipeline is less than the temperature change needed to form the pre-melting layer, and hence hydrate begins to grow as expected. Once the pipeline temperature drop is less than the temperature drop needed for the quasi-liquid layer to form hydrate particles come together, and hydrate growth occurs.

Table 1. Fluid and System Properties for XY Field.

Properties	Value
Gas – Condensate Ratio (scf/stb)	250
Water Cut	0.23
Condensate Density (kg/m <sup>3</sup> )	879.2
Gas Density (kg/m <sup>3</sup> )	161.8
Water Density (kg/m <sup>3</sup> )	1013.5
Mass rate total ((kg/s)	29.23
Gas Specific Gravity	0.75
Oil Specific Gravity	0.88
Specific heat capacity of water (kJ/kg K)	4.186
Specific heat capacity of gas (kJ/kg K)	2.22
Specific heat capacity of hydrates	2.75
Initial Temperature (°C)	26.93

Table 2. Parameters for Quasi Liquid Layer Temperature.

Parameter	Value
$\dot{m}_{gas}$ (kg/s)	28.34
$\dot{m}_{water}$ (kg/s)	0.20
$\dot{m}_{condensate}$ (kg/s)	0.46
$\alpha_{hydrate}$ (%)	0.78
$\rho_{hydrate}$ (kg/m <sup>3</sup> )	910
$u_{hydrate}$ (m/s)	0.67

Table 3. Changes in Pipeline that quasi liquid layer will form.

Length of Pipeline (ft)	Temperature (°K)	Time (t) (Seconds)	$\Delta T_P$ (°K)	$\Delta T_Q$ (°K)	Remarks
0	26.93	-	-	-	
200	15.84	300	11.09	5.14	
400	9.50	600	17.43	10.28	$\Delta T_P > \Delta T_Q$
600	5.86	900	21.07	15.43	No Formation of
800	3.78	1200	23.15	20.58	Pre-melting Layer
1000	2.59	1500	24.34	25.72	
1200	1.91	1800	25.02	30.86	
1400	1.52	2100	25.41	36.00	
1600	1.30	2400	25.63	41.15	$\Delta T_P < \Delta T_Q$
1800	1.17	2700	25.76	46.29	Starting Point of
2000	1.10	3000	25.83	51.44	Pre-melting Layer
2200	1.06	3300	25.87	56.58	Formation
2400	1.03	3600	25.90	61.72	
2600	1.02	3900	25.91	66.87	

## 4. Conclusion

In this work, we developed an analytical correlation to predict the temperature at which a quasi-liquid (also known as a pre-melting layer) would be formed. The model extensively dealt with the energies involved in hydrate formation, Gibb's free energy to the mass transfer that occurs during hydrate growth, and microscopic energy balance and mass balance of crystal formation to predict the temperature at which a quasi-liquid or pre-melting layer would be formed. The pre-melting temperature is a function of the pipeline length, time for the fluid to flow in the system, hydrate density, change in enthalpy, flowing hydrate velocity, percentage of hydrate in fluid composition.

The developed correlation will help to identify when heating of pipelines can be done to control hydrate formation in a bid to keep the temperature above the quasi-liquid layer temperature. Also, since, thermal inhibition of hydrates, just like chemical inhibition is very expensive and in some cases not environmentally friendly. This developed model can identify the point where thermal inhibition should be started thereby making hydrate formation control more cost-effective.

The empirical constants B and R should be experimentally determined for future work.

## References

- [1] Irfan Kurawle, Mohit Kaul, Zoab Amin, Nikhil Kulkarni. (2008). Semi-Analytical Study of Production of Gas Hydrates and Their Techno-Economic Uses. SPE, Maharashtra Institute of Technology, Pune. This paper was presented at the International Petroleum Technology Conference held in Kuala Lumpur, Malaysia, 3–5 December.
- [2] Sloan E. Dendy, Koh Carolyn Ann. (2008). Clathrate hydrates of natural gases. Third edition. CRC Press, 6000 Broken Sound Parkway NW, Suite 300, Boca Raton, Florida 33487-2742, U.S.A.
- [3] Steed Jonathan W, Atwood Jerry L. (2013). Supramolecular Chemistry. 2nd edition, Wiley.
- [4] Sloan E. Dendy, Koh Carolyn Ann, Sum K. Amadeu, Ballard A. L., Shoup, G. J... & Palermo Thierry. (2009). Hydrates: State of the Art Inside and Outside Flow lines. *Journal of Petroleum Technology* 61 (12): 89-94. doi: 10.2118/118534-MS.
- [5] Haghghi H., Azarinezhad R., Chapoy A., Anderson R., Tohidi B. (2007). Hydraflow: Avoiding Gas Hydrate Problems, SPE 107335, 11th-14th June, London, United Kingdom. doi.org/10.2118/107335-MS.
- [6] Akinsete Oluwatoyin Olakunle, Isehunwa Sunday Oloruntoba (2015). Novel Analytical Model for Predicting Hydrate Formation Onset Pressures in Natural Gas Pipeline Systems. *Journal of Characterization and Development of Novel Materials* 7 (4): 605-619.
- [7] Sum K. Amadeu, Koh Carolyn Ann, Sloan E. Dendy. (2009). Clathrate Hydrates: From Laboratory Science to Engineering Practice. *Industrial & Engineering Chemistry Research*. 48 (16): 7457–7465. <https://doi.org/10.1021/ie900679m>
- [8] Sloan E Dendy. (2003). Clathrate hydrate measurements: Microscopic, mesoscopic, and macroscopic. *The Journal of Chemical Thermodynamics*. 35: 41-53. doi: 10.1016/S0021-9614(02)00302-6.
- [9] Yoslim Jeffry, Linga Praveen, Englezos Peter. (2010). Enhanced Growth of Methane Propane Clathrate Hydrate Crystals with Sodium Dodecyl Sulfate, Sodium Tetradecyl Sulfate, and Sodium Hexadecyl Sulfate Surfactants. *Journal of Crystal Growth* 313 (1): 68-80. doi: 10.1016/j.jcrysgro.2010.10.009.
- [10] Englezos P., Kalogerakis, N., Dholabhai, P. D. and Bishnoi, P. R. (1987). Kinetics of formation of methane and ethane gas hydrates, *Chemical Engineering Science*, 42 (11): 2647-2658. doi: 10.1016/0009-2509(87)87015-X.
- [11] Yimin Li, Gabor A. Somorjai. (2007). Surface premelting of ice. *The Journal of Physical Chemistry*. 111 (27): 9631–9637. doi.org/10.1021/jp071102f.
- [12] Kazunori Okutani, Yui Kuwabara, Yasuhiko H. Mor. (2008). Surfactant Effects on Hydrate Formation in an Unstirred Gas/Liquid System: An Experimental Study Using Methane and Sodium Alkyl Sulfates, *Chemical Engineering Science*, 63 (1): 183-194. doi.org/10.1016/j.ces.2007.09.012.
- [13] Huo Z., Freer E., Lamar M., Sannigrahi B., Knauss D. M., Sloan E. D. (2001). Hydrate plug prevention by anti-agglomeration. *Chemical Engineering Science*. 56 (17): 4979–4991.
- [14] Nobuo Maeda. (2015). Is the Surface of Gas Hydrates Dry? *Energies*. 8 (6): 5361-5369; doi: 10.3390/en8065361.
- [15] Peidong Yang (2016). Materials & Solid State Chemistry (course notes). UC Berkeley. Chemistry 253.
- [16] Bishop C. L., Pan D., Liu L. M., Tribello G. A., Michaelides A., Wang E. G., Slater B. (2009). On thin ice: Surface order and disorder during pre-melting. *Faraday discussions* 141: 277–292. <https://doi.org/10.1039/B807377P>
- [17] Talaghat Mohammad Reza, Jekar Seyyed Mohammad. (2018). Prediction of induction time for methane hydrate formation in the presence or absence of THF in flow loop system by Natarajan model. *Heat Mass Transfer* 54: 2783–2792. <https://doi.org/10.1007/s00231-017-2263-5>
- [18] Bravais class. Online Dictionary of Crystallography. IUCr. Retrieved 8 August 2019.
- [19] Dimo Kashchiev, Abbas Firoozabadi. (2003). Induction time in crystallization of gas hydrates. *Journal of Crystal Growth*, 250 (3–4): 499-515. doi.org/10.1016/S0022-0248(02)02461-2.
- [20] Englezos Peter, Bishnoi P. Raj (1988). Gibbs free energy analysis for the supersaturation limits of methane in liquid water and the hydrate-gas-liquid water phase behavior. *Fluid Phase Equilibria*. 42: 129-140. doi.org/10.1016/0378-3812(88)80054-2.
- [21] Bishnoi P. Raj, Natarajan V. (1996). Formation and decomposition of gas hydrates. *Fluid Phase Equilibria*. 117 (1–2): 168-177, ISSN 0378-3812. doi.org/10.1016/0378-3812(95)02950-8.
- [22] Leach Sydney. (2014). Size effects on cation heats of formation. III. Methyl and ethyl substitutions in group IV XH<sub>4</sub>, X = C, Si, Ge, Sn, Pb. *The journal of physical chemistry* 118 (48): 11417-31. doi.org/10.1021/jp509468z.
- [23] Vinatovskaja, E. 2015. Cold Flow in the Arctic: A Feasibility Study. Master Thesis, University of Stavanger, Stavanger.